



Power Electronic Systems
Laboratory

© 2014 IEEE

Proceedings of the IEEE Energy Conversion Congress and Exposition (ECCE USA 2014), Pittsburgh, Pennsylvania, USA, September 14-18, 2014

Volume/Weight/Cost Comparison of a 1MVA 10 kV/400V Solid-State against a Conventional Low-Frequency Distribution Transformer

J. Huber,
J. W. Kolar

This material is published in order to provide access to research results of the Power Electronic Systems Laboratory / D-ITET / ETH Zurich. Internal or personal use of this material is permitted. However, permission to reprint/republish this material for advertising or promotional purposes or for creating new collective works for resale or redistribution must be obtained from the copyright holder. By choosing to view this document, you agree to all provisions of the copyright laws protecting it.



Eidgenössische Technische Hochschule Zürich
Swiss Federal Institute of Technology Zurich

Volume/Weight/Cost Comparison of a 1 MVA 10 kV/400 V Solid-State against a Conventional Low-Frequency Distribution Transformer

Jonas E. Huber and Johann W. Kolar

Power Electronic Systems Laboratory
ETH Zurich
8092 Zurich, Switzerland
huber@lem.ee.ethz.ch

Abstract—Solid-State Transformers (SSTs) are an emergent topic in the context of the Smart Grid paradigm, where SSTs could replace conventional passive transformers to add flexibility and controllability, such as power routing capabilities or reactive power compensation, to the grid. This paper presents a comparison of a 1000 kVA three-phase, low-frequency distribution transformer (LFT) and an equally rated SST, with respect to volume, weight, losses, and material costs, where the corresponding data of the SST is partly based on a full-scale prototype design. It is found that the SST’s costs are at least five times and its losses about three times higher, its weight similar but its volume reduced to less than 80 %. In addition, an AC/DC application is also considered, where the comparison turns out in favor of the SST-based concept, since its losses are only about half compared to the LFT-based system, and the volume and the weight are reduced to about one third, whereas the material costs advantage of the LFT is much less pronounced.

I. INTRODUCTION

In today’s distribution grids, conventional low-frequency transformers (LFTs) are ubiquitous at the interfaces between different voltage levels, where they provide voltage scaling and galvanic isolation. Because of the low operating frequency of 50 Hz or 60 Hz, LFTs are usually large and heavy devices. Their low complexity and passive nature is a benefit (high reliability) and a downside (no control possibilities) at the same time. The latter is increasingly important in the scope of recent developments such as the propagation of distributed generation systems on lower voltage levels and the Smart Grid paradigm in general, which implies a high degree of controllability of loads and also power flows. Controllability, however, is an inherent feature of power electronic converter systems, which have found their application in grid-related systems such as for example FACTS and STATCOMs. While these technologies can enhance the functionality of passive LFTs, they do not replace them.

The next logical step is thus to completely substitute LFTs by so-called Solid-State Transformers (SSTs), which interface the grids on either side through power electronic converters and provide galvanic isolation by means of medium-frequency transformers (cf. Fig. 1(b)). The first “electronic transformer”

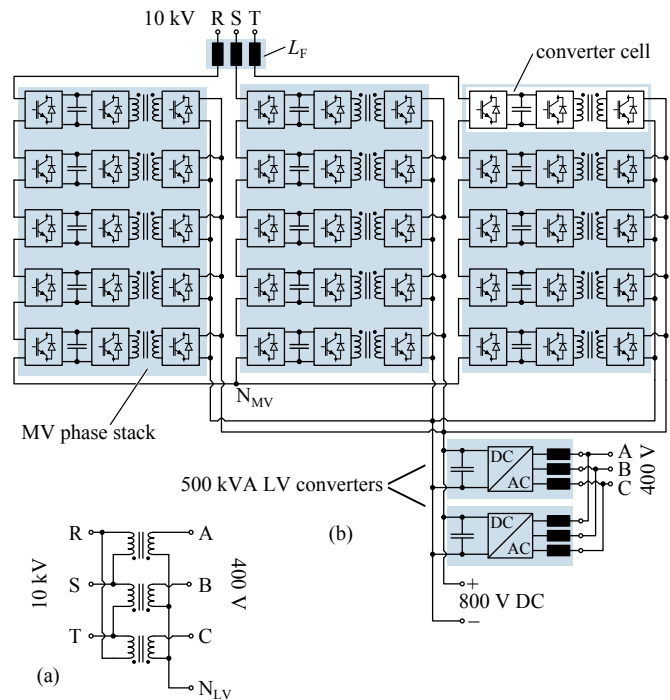


Fig. 1. Schematic of a delta-wye connected LFT (a), and basic structure of the SST circuit topology considered throughout this work (b), which comprises an isolated 1000 kVA cascaded MV AC to LV DC converter (cf. Fig. 3(a) for a detailed schematic of the converter cells’ power circuits) and, depending on the application, two 500 kVA LV DC to LV AC converters.

has been patented already in the early 1970ies [1], but it took almost three decades until the concept was seriously considered for grid level ratings around the onset of the 21st century [2]–[6]. Whereas this paper focuses on grid applications, SSTs are also proposed for traction systems [7]–[10], where a reduction in size and weight as well as an efficiency increase can be achieved as a result of the medium-frequency potential separation, which is highly beneficial especially in distributed traction systems.

Commonly, reductions in size and weight are projected for

changing from an LFT to an equally rated SST. However, whereas for traction systems a weight reduction of around 50 % at a 50 % higher price tag has been reported based on a 1.5 MVA prototype [11], literature provides only vague data for grid applications. In [12], a cost increase by a factor of ten is mentioned for grid-scale SSTs and small quantity production and [13] describes the optimization of a 150 kVA high-frequency transformer for SSTs with respect to weight, volume and cost. A multi-dimensional comparison of cascaded converter designs with different numbers of levels for direct grid connection of wind turbines is described in [14], however, only power semiconductor costs are considered. Looking at lower power levels, [15] compares the cost of four different topologies suitable for a 50 kVA SST's high-voltage side converter and [16] provides a cost breakdown of a laboratory-scale prototype of an SST for wind energy applications and, as a side note, mentions an estimated cost reduction by a factor of five when moving from the laboratory prototype to series production. Recently, a single-phase, 13.8 kV/270 V SST based on silicon carbide (SiC) devices rated at 10 kV blocking voltage has been presented, apparently achieving a 75 % reduction in weight and a 40 % reduction in size compared with a conventional single-phase LFT [17]. However, for the time being, and probably also for several years to come, the industrial heavy-duty converter population is and likely will be dominated by proven and relatively lower cost silicon technology.

Although, as has been tried to outline, research efforts in the SST area are diverse and exciting, no direct quantitative comparison of a fully rated three-phase AC/AC SST and a corresponding LFT has been reported so far. This paper presents such a comparison of an exemplary 1000 kVA, 10 kV/400 V LFT, which is a typical unit rating found in European distribution systems, and an equally rated SST with respect to four key performance characteristics: weight, volume, material costs, and losses. The LV DC bus of the SST structure shown in Fig. 1(b) can interface DC microgrids, e. g., in buildings, or also DC generators such as photovoltaics. Since such DC applications are becoming more and more important, scenarios where the LV side output of the transformer involves 50 % or 100 % DC power are also considered in the comparison.

Material costs are estimated here by means of component cost models for high-volume production as proposed in [18], i. e., it is important to highlight that all costs mentioned throughout this paper comprise only material costs and hence are to be understood as lower bounds, not including labor costs, profits, etc. In addition, this approach implies that only hardware costs are considered. In power systems engineering, however, usually a total cost of ownership (TCO) perspective is taken when evaluating the economical aspect of, e. g., equipment to reduce power quality issues [19], distribution system enhancement projects [20] or smart substations [21]. Therefore, this paper should be viewed as a first step towards a comprehensive quantitative comparison of the costs of an SST and an LFT. The scope of the analysis presented here needs to be broadened in the future and the complete system consisting of the SST and the associated grid section should

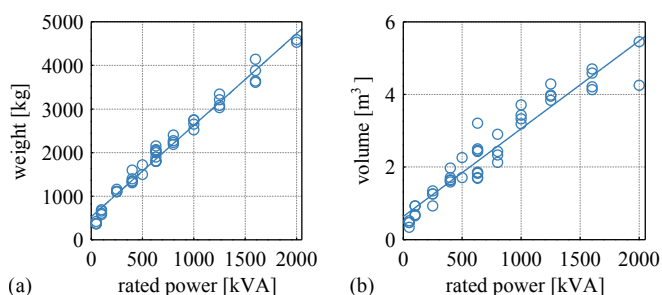


Fig. 2. Dependence of LFT weight (a) and volume (b) on the rated power; based on datasheet information from [22].

be taken into account whenever possible.

The paper is structured as follows: Sections II and III describe reference LFT data and the modeling of the SST, respectively, and Section IV provides the results of the comparison between SST and LFT for different application scenarios as well as a discussion of these results.

II. LFT PERFORMANCE CHARACTERISTICS

Fig. 1(a) shows the basic schematic of a three-phase LFT in delta-wye connection. The electrical part consists of two times three copper (or aluminum) windings and a magnetic core, which is usually made of low-loss silicon steel laminations. While dry-type solutions are available, distribution transformers with higher power ratings are typically immersed in oil to provide both, isolation and cooling.

Fig. 2 illustrates the largely linear dependency of weight and volume, respectively, on the rated power, based on data of a wide range of distribution transformers given in [22]. Usually, different transformer variants are available for a given power rating, which differ in their part load and full load efficiencies. This translates into different weights and sizes, since more or less active material, i. e., copper and silicon steel, is used. Consequently, a trade-off between purchase price and the cost of loss energy arising during the transformer's lifetime exists and an optimization can be performed, which is done within a so-called total cost of ownership (TCO) analysis.

Looking specifically at 1000 kVA units, datasheets of various manufacturers provide dimension, weight and loss information [22]–[24]. Averaging those values yields the volume and weight of a typical 1000 kVA LFT as 3.43 m³ (4.48 yd³) and 2590 kg (5710 lb), respectively, and an average full-load efficiency of 98.7 %. Note that the full-load efficiencies of the considered units vary between 98.5 % and 98.9 %, which is, however, not really relevant compared to the efficiency difference to an AC/AC SST, as is to be discussed later.

The purchase price of a typical 1000 kVA distribution transformer is given as 16 kUSD in [25], and as 12 kEUR in [26], which corresponds to 16.2 kUSD (as of June 2014). Depending on the optimization target, as discussed above, prices may vary about ± 35 % around this mean value. These numbers are also in agreement with pricing information obtained from a major European transformer manufacturer. According to [26],

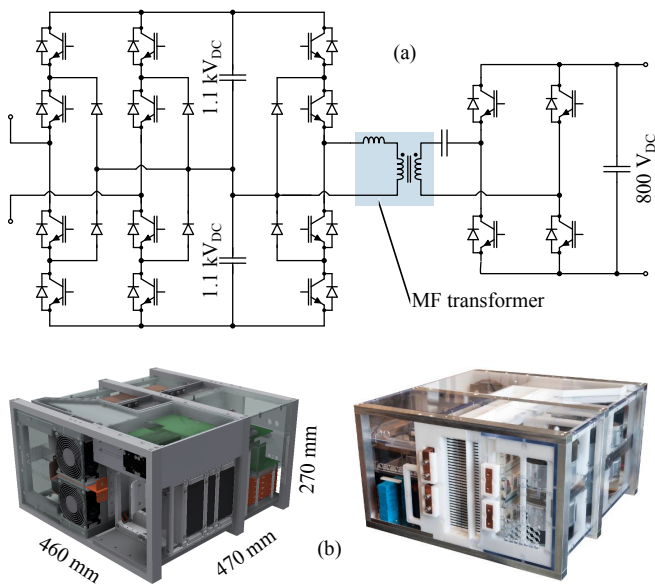


Fig. 3. Power circuit of one converter cell used in the SST's MV side phase stack (a), and 3D CAD rendering and photo of a corresponding fully rated, 85 kW prototype (b).

active material costs account for 50% and overall material costs for 70% of the transformer price. Thus, overall material costs of roughly 11.3 kUSD can be assumed for the exemplary 1000 kVA unit.

III. SST PERFORMANCE CHARACTERISTICS

While LFTs can be purchased off-the-shelf, no SST products do exist so far. Therefore, the four performance characteristics (weight, volume, material costs, and losses) of an exemplary SST realization are derived in this section, partly based on a hardware prototype.

Fig. 1(b) shows the basic schematic of the considered SST circuit topology. The SST interfaces the medium-voltage (MV) grid through a cascaded cells converter system, where each of the cascaded converter cells (cf. Fig. 3(a)) features an isolated DC/DC converter, providing galvanic isolation by means of a medium-frequency transformer. Fig. 4(a) shows the MV converter's multilevel output voltage and the resulting grid current at full-load operation.

On their low-voltage (LV) side, all cells are connected to a common DC bus, which feeds two paralleled 500 kVA, three-phase converters connected to the LV grid. Again, Fig. 4(b) shows the output voltage and the corresponding grid current for one of the two 500 kVA units.

The cascaded MV side converter and the three-phase LV converter are discussed separately in the following two subsections, whereby, for the sake of brevity and clarity, the reader is referred to references for details on the models used.

A. Medium-Voltage Side Cascaded Converter

Since today's Si power semiconductors are not available with blocking voltage ratings above 6.5 kV, cascading of converter

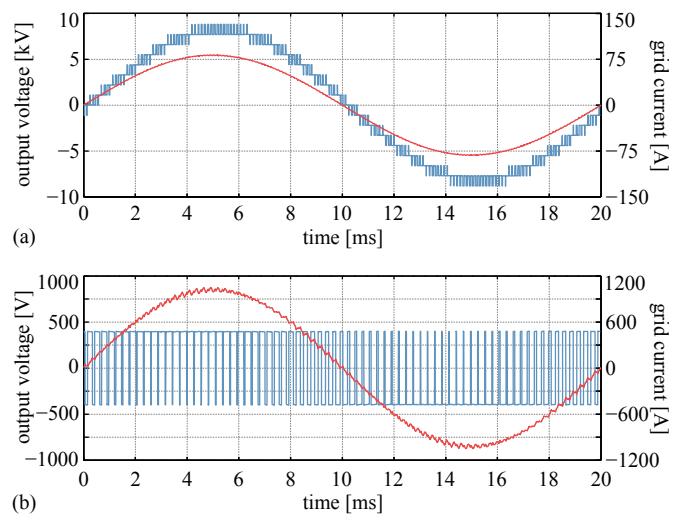


Fig. 4. MV side output voltage and resulting line current for (a) the cascaded 1000 kVA MV converter, and (b) corresponding LV side waveforms for one of the 500 kVA LV converter units (cf. Fig. 1(b)) for full-load active power operation.

cells becomes necessary when interfacing a 10 kV MV grid (cf. Fig. 1(a)). In addition, cascading offers a multilevel output voltage waveform (cf. Fig. 4(a)), reducing filtering efforts, and provides modularity and redundancy. The converter considered here uses five cascaded cells (per MV phase) based on NPC bridge legs and 1700 V IGBTs on their MV side, which have been found to offer a good trade-off between efficiency and power density for this voltage and power range [27]. Note that one cell per phase stack serves only redundancy purposes and is not active during normal operation, i.e., it contributes to weight, volume and costs, but not to losses.

The power circuit of one converter cell is given in Fig. 3(a), Fig. 3(b) shows a 3D CAD rendering and a photo of the corresponding fully rated 85 kW prototype, which is currently under construction at the Power Electronic Systems Laboratory of ETH Zurich, and Table I gives an overview on the major specifications. Each cell features a single-phase, five-level inverter/rectifier stage and an isolated DC/DC converter, which is realized as a half-cycle discontinuous-conduction-mode series-resonant-converter (HC-DCM-SRC) [28], [29]. Its medium-frequency transformer is made of nanocrystalline core material and Litz wire windings.

Based on the converter cell prototype, volume and weight of a single cell can directly be obtained. The costs of the main components are determined using cost models for high-volume production as presented in [18], however the cost model for the medium-frequency transformer has been adjusted by considering material costs only and adding a 50% premium to account for the rather complicated, when compared to standard inductive components, isolation and cooling system.

The line filter inductors, L_F , are designed by means of thermally limited volume vs. loss Pareto optimization on the basis of laminated steel UI-cores and solid copper windings. The core dimensions are varied over a wide range to obtain

TABLE I
MAIN SST PARAMETER AND COMPONENTS OVERVIEW.

MV filter inductor, L_F	25 mH
Cell AC/DC stage devices	150 A/1700 V IGBTs
Cell AC/DC stage sw. freq.	1 kHz
Cell MV DC link voltage	2×1100 V
Cell MV DC link capacitors	2×750 μ F, film
Cell DC/DC stage MV devices	150 A/1700 V IGBTs
Cell DC/DC stage sw. freq.	7 kHz
Cell DC/DC stage LV devices	200 A/1200 V IGBTs
Cell LV DC link voltage	800 V
Cell LV DC link capacitor	250 μ F, film
LV inverter DC link capacitors	2×7 mF
LV inverter devices	1.2 kA/1200 V IGBTs
LV inverter sw. freq.	3.6 kHz
LV inverter boost inductor, L_B	345 μ H

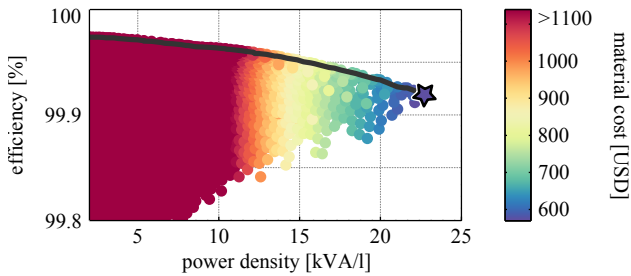


Fig. 5. Pareto optimization of the MV filter inductors with the chosen design highlighted.

a high number of designs, which can then be plotted in the efficiency/power density plane as done in Fig. 5, where the chosen design on the Pareto front is highlighted. Costs are again estimated using the material cost part of the inductor cost models given in [18].

Using datasheet characteristics for conduction and switching losses, the AC/DC stage efficiency has been calculated and together with the losses of the optimized filter inductors and an estimated DC/DC converter efficiency of 99%, which is typically feasible with this kind of soft-switching DC/DC converters [30], the overall MV side (i. e., from three-phase MV AC to LV DC) converter efficiency is obtained as 98.2%.

The volume of a converter cell is given by the prototype design and that of the filter inductor's bounding box follows from the optimization. The overall MV side converter volume can therefore be obtained as the sum of fifteen times the cell volume and three times the inductor volume. In addition, a volume utilization factor of $u_V = 0.75$ is assumed to account for empty spaces inevitably found in practical assemblies, i. e., the total volume is given as

$$V_{\text{total}} = \frac{1}{u_V} \sum_{i=1}^n V_{\text{component},i}. \quad (1)$$

Of course, the SST's power electronics needs to be contained in cabinets. Therefore, Fig. 6 shows the dependencies of cabinet weight and cost on the enclosed volume, i. e., V_{total} . Cabinet dimension and weight data is taken from a manufacturer's

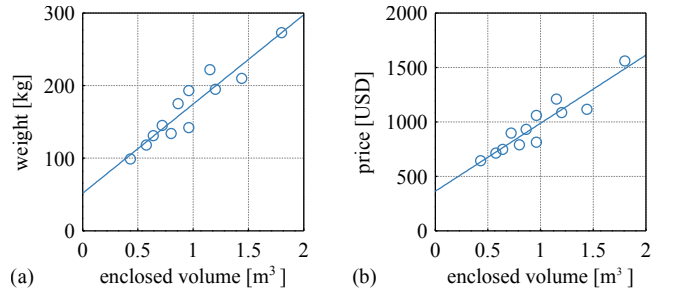


Fig. 6. Dependence of cabinet weight (a) and price (b) on the enclosed volume.

TABLE II
PERFORMANCE CHARACTERISTICS OVERVIEW (TWO 500 kVA UNITS ARE CONSIDERED FOR THE LV SIDE).

	SST MV	SST LV	SST	LFT
Efficiency [%]	98.3	98.0	96.3	98.7
Volume [m ³]	1.57	1.10	2.67	3.43
Weight [kg]	1270	1330	2600	2590
Mat. cost [kUSD]	34.1	18.6	52.7	11.4

brochure [31], whereas price information is obtained from a large distributor. Thus, additional weight and cost contributions from the converter housing can be included in the corresponding estimates.

The resulting performance characteristics for the SST's MV side converter are summarized in Table II, while Fig. 10(a) and (d) present weight and cost breakdowns, respectively.

B. Low-Voltage Side Converter

As can be seen from the SST structure shown in Fig. 1(a), the LV side three-phase inverter part is split into two parallel connected 500 kVA units to improve flexibility. Fig. 7 shows the power circuit considered for the optimization of one of these 500 kVA units and Table I gives an overview on the main parameters resulting from the optimization described in the following.

The design of such standard three-phase systems is well documented in literature and analytic expressions for all semiconductor currents and, together with datasheet characteristics, device losses are available [32]. The DC link capacitor volume is modeled assuming a constant energy density of 6.3 cm³/J for film capacitors, which is based on datasheet averaging. Forced-air cooling is assumed and the corresponding heatsink volume

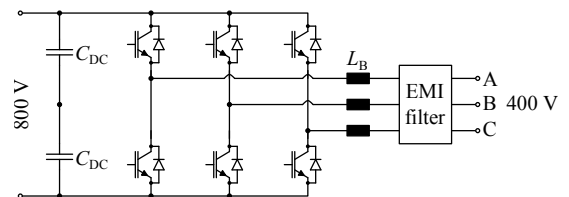


Fig. 7. Power circuit of the LV inverter stage.

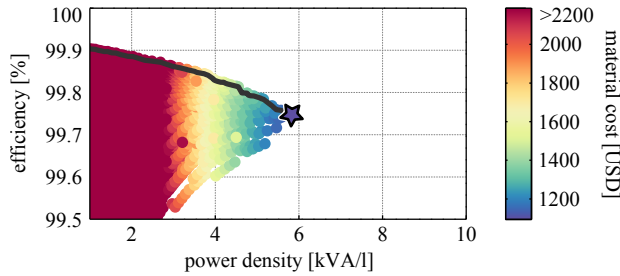


Fig. 8. Pareto optimization of the LV filter inductors with the chosen design highlighted. Due to the very high currents, the achievable power densities are significantly lower than in the MV case.

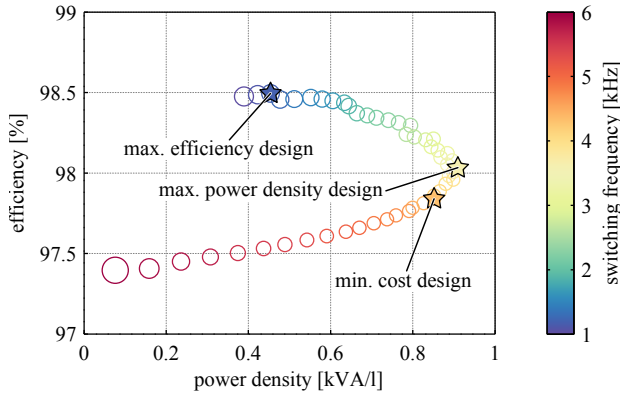


Fig. 9. Different design variants of a 500kVA LV converter for 10% peak-to-peak current ripple and different switching frequencies. The size of the circles indicates the designs' material costs.

is estimated using a Cooling System Performance Index (CSPI) [33] of 10 W/K dm^3 (0.164 W/K in^3), 50°C ambient and 125°C maximum junction temperature. The boost inductors, L_B , are optimized as described above for the MV side filter inductors and the result is shown in Fig. 8. Thus, the overall weight and the overall volume—here employing a volume usage factor of $u_V = 0.25$ as a more conservative value for large, conventional power converters—of a given design can be estimated as well as costs can be modeled using [18] again.

To identify an optimum overall design, an efficiency vs. power density Pareto optimization is employed. For a given maximum peak-to-peak output current ripple specification of 10%, the switching frequency is varied and the required boost inductance, L_B , adjusted accordingly [34]. The resulting designs can be plotted in the efficiency vs. power density plane as shown in Fig. 9, where the cost information is provided in the figure by the size of the circles. Three different optimization targets can be identified: maximum efficiency, maximum power density and minimum cost; all of which are highlighted in the figure. The maximum power density design is considered for the comparison with the LFT, because it features still a comparatively high efficiency and its material costs are not significantly higher when compared with the minimum cost design. The related performance characteristics of the SST's LV side converter can be found in Table II, and Fig. 10(b) and

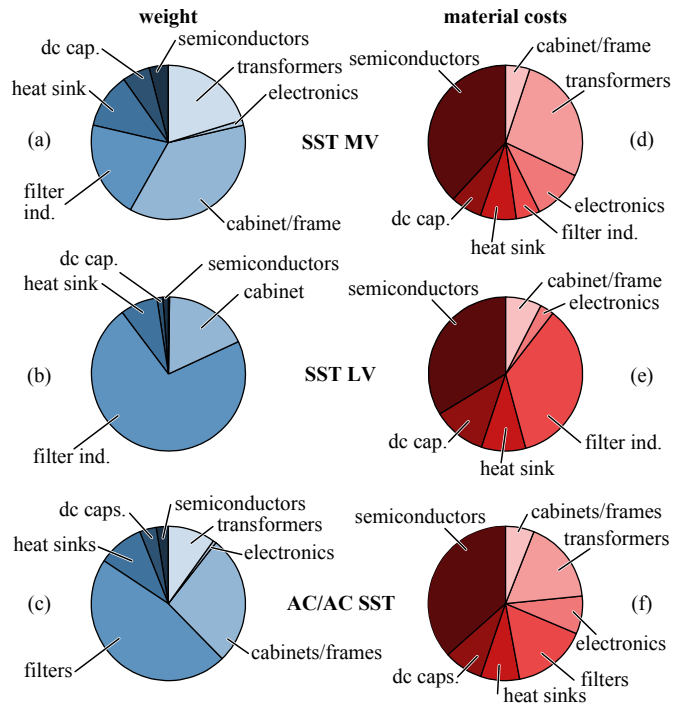


Fig. 10. Weight breakdowns of the MV converter (a), the LV converter (b) and the complete AC/AC SST (c); material cost breakdowns of the MV converter (d), the LV converter (e) and the complete AC/AC SST (f).

(e) show corresponding weight and loss breakdowns.

To support the results of this rather coarse modeling procedure, they are briefly compared with a 540kVA active front end converter of a commercially available high-power drive system [35], i. e., a converter very similar to the one discussed here. First, this is a good opportunity to highlight again that the cost discussion here is limited to material cost estimates. The list price of the said active frontend converter is around 64 kUSD [36], which is almost seven times the material costs estimated here. Reasons for this difference are likely to be found in engineering and manufacturing costs, warehousing, amortizations, marketing and price policies, etc., which are hard to model. Regarding the other three performance characteristics, i. e., mass, efficiency, and volume, the calculated values of the 500kVA LV unit are within $\pm 10\%$ of the values reported for the said 540kVA active front end converter, indicating that despite neglecting many auxiliary components such as breakers, busbars, etc., still a fairly accurate estimate of these three performance characteristics can be obtained.

C. SST Weight and Cost Structure

Fig. 10 shows the weight and material cost structures of the MV converter, the LV converter, and, combining them, the overall 1000kVA AC/AC SST. It is interesting to notice that still the low-frequency magnetic components, i. e., the filter inductors, contribute a major share to weight and, especially in the case of the LV converter, where the phase currents are very high and consequently the required amount of copper conductor material is high as well, also to material costs. Hence,

TABLE III
CHARACTERISTIC PERFORMANCE INDICES FOR 1000kVA LFT-BASED AND SST-BASED SOLUTIONS IN AC/AC OR AC/DC APPLICATIONS.

	AC/AC			AC/DC		
	LFT	factor	SST	LFT	factor	SST
Losses [W/kVA]	13.0	$\times 2.87$	37.3	32.7	$\times 0.53$	17.3
Costs [USD/kVA]	11.4	$\times 4.61$	52.7	30.0	$\times 1.14$	34.1
Volume [l/kVA]	3.4	$\times 0.78$	2.7	4.5	$\times 0.35$	1.6
Weight [kg/kVA]	2.6	$\times 1.00$	2.6	3.9	$\times 0.32$	1.3

these passive filter components are of particular interest in order to further cut costs and weight of SSTs. They could be reduced in volume by increasing the switching frequency, which is, however, not feasible with today's power semiconductors' high switching losses, as is illustrated in Fig. 9. Nevertheless, emerging technologies such as silicon carbide (SiC) can be expected to significantly contribute to further weight reduction through higher switching frequencies and consequently reduced sizes of passives. It is this context in which the higher costs of new technologies such as SiC power devices need to be considered on a system-oriented basis.

Other important contributions to material costs are the medium-frequency transformers and the power semiconductors. The cascaded MV converter also requires quite complex control and communication electronics, therefore their share of the overall costs is clearly higher than in the LV converter.

IV. COMPARISONS

With the four performance characteristics now determined for both, a typical 1000kVA LFT and an equally rated, exemplary SST, the two concepts can be compared, first for the classical AC/AC use-case and second for two more modern AC/DC applications.

A. AC/AC Applications

Here, an AC/AC scenario is considered in which the SST directly replaces an LFT as the interface between a three-phase MV and a three-phase LV grid. Fig. 11(a) compares the two cases, where material costs, mass, volume and losses are normalized to the LFT solution. In addition, Table III presents the comparison results in terms of four performance indices: losses per kVA, material costs per kVA, volume per kVA and weight per kVA. The SST solution is about a factor of five more expensive, produces roughly three times higher losses, has similar weight but uses only 80% of the LFT's volume.

B. AC/DC Applications

Nowadays, local low-voltage DC systems are coming back in focus for in-building or in-factory power distribution, but also for entire DC microgrids, since many loads (e. g., drives, computers, lighting, etc.) and also generators (e. g., photovoltaics) are essentially devices featuring a DC port. Therefore, the second use-case for an SST is at the interface between a three-phase MV grid and a low-voltage DC distribution system.

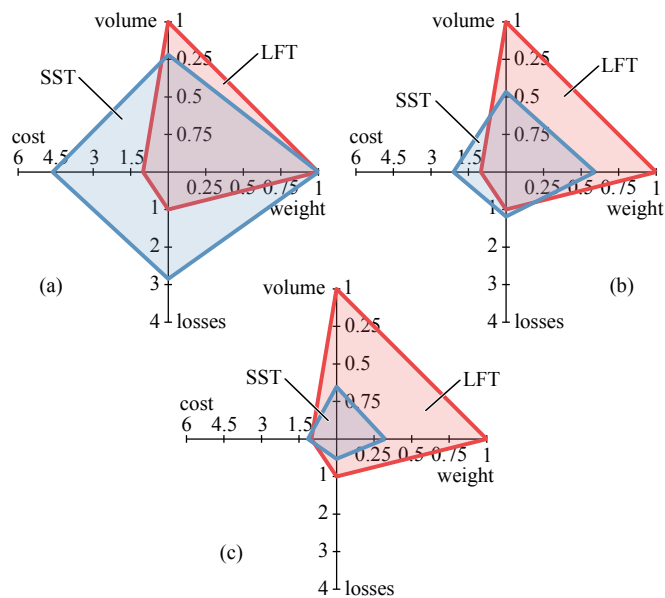


Fig. 11. Comparison of LFT and SST performance characteristics, normalized to the LFT solutions, (a) for AC/AC operation, (b) for 50% AC/AC and 50% AC/DC operation, and (c) for AC/DC operation. Note that the material costs estimate for the SST solutions constitutes a lower bound only.

1) *Mixed 50% LV DC, 50% LV AC*: First, a mixed environment where 50% of the rated power needs to be provided as LV DC and the other 50% as standard three-phase LV AC is looked at. The SST thus consists of the 1000kVA MV converter part and one of the 500kVA LV converters (cf. Fig. 1(b)), whereas the LFT-based solution extends the LFT also by one of the 500kVA units to act as a rectifier.

Fig. 11(b) compares the two approaches. With respect to the pure AC/AC case, the SST-based solution compares much more favorable in this mixed scenario. Note that the modularity of the SST system allows for a variety of different nominal LV AC and DC power ratings, since, e. g., instead of one 500kVA unit also three 250kVA units could be employed, etc.

2) *100% LV DC*: Finally, a pure AC/DC application is considered, where the SST solution is reduced to the MV converter part and on the other hand the LFT needs to be extended by two 500kVA rectifier/inverter units.

The resulting comparison between the SST-based and the LFT-based solution is given in Fig. 11(c) and the absolute data in terms of performance indices can again be found in Table III. Here, the SST solution outperforms the LFT-based solution in all areas except costs: it uses only one third of the LFT-based solution's volume, has only one third of the weight, and produces only about half the losses.

The latter is illustrated by Fig. 12, where the loss distributions for the three cases are shown. The SST's cascaded MV side converter can transform from three-phase MV AC to LV DC at an efficiency already close to that of the LFT. Accordingly, once an LV DC output is required and thus the LFT's LV AC output needs to be rectified, the resulting LFT-based system's efficiency cannot compete anymore. Furthermore, it should

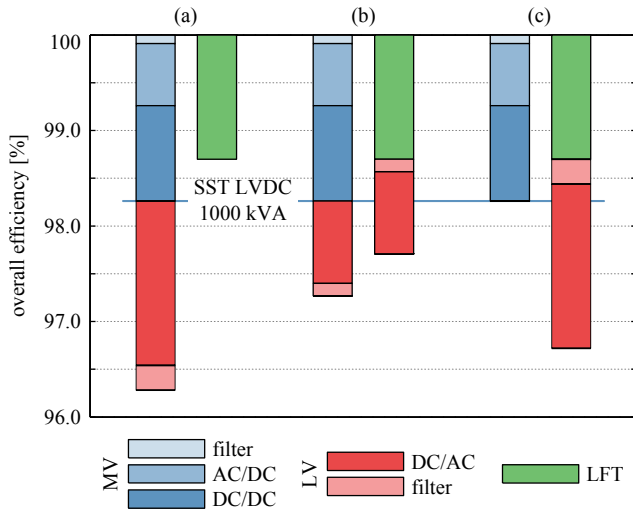


Fig. 12. Loss distribution of the three considered application cases, where (a) is for full AC/AC operation, (b) is for 50% AC/DC and 50% AC/AC operation, and (c) is for full AC/DC operation. Note that overall system losses at full-load operation, i. e., where AC and DC outputs are loaded with their respective rated power, are considered.

TABLE IV
SPECIFIC RESSOURCE USAGE.

	SST MV	SST LV	AC/AC SST	LFT (est.)
kg Cu/kVA	0.15	0.32	0.47	0.6
kg Fe/kVA	0.32	0.63	0.95	1.2
mm ² Si/kVA	85	22	107	0

be mentioned that in the AC/DC case the same limitations regarding overload capability apply for both solutions, whereas in the AC/AC application a power electronics system cannot compete with the short-term overload capacity of an LFT.

C. Resource Usage

Environmental concerns are one of the main driving forces behind power electronics and thus also SST research—consider for example the oil-free design of SSTs. Therefore, resource usage is an aspect that should be looked at next to efficiency, too. Table IV gives an overview on the consumption of copper, iron core material, and silicon per kVA of rated power for the SST, its LV and MV converters, and the LFT. The values for the SST systems can be obtained from the modeling results described above; for the LFT an estimate based on the total weight and the oil mass of 1000 kVA units as given in [22] has been calculated by assuming a 3 mm thick steel enclosure and a typical, according to [25], ratio of core to copper weight of 2:1.

As expected, the specific consumption of active metals in the SST can be reduced by about one fourth compared to the LFT. What is even more interesting is the comparison between the MV side and the LV side converter systems: The cascaded MV side converter requires a high number of power semiconductors to generate a very high quality output voltage waveform, thus reducing the required filter size. While the MV

converter’s specific usage of copper and core material therefore is only about half the LV converter’s (even though the MV stage contains also the DC/DC converters’ transformers), this is paid by a fourfold increase in required silicon area, which reflects exactly the different topologies used.

D. Discussion

The presented analysis indicates that SST technology will have a hard time competing with well proven distribution transformer technologies in classic AC/AC applications, i. e., replacing an LFT by an SST might not be feasible. Efficiencies of SSTs will remain significantly lower than those of LFTs in the AC/AC case. It should be noted that the LFT material costs are derived from price data of ready-to-buy units, whereas SST material costs are estimated for exemplary prototype designs and rely on component cost models for the main power components only and do not include, e. g., protection equipment, final assembly costs, profit margins or installation costs, although the latter can be expected to be comparatively low due to the SST’s modular nature. Nevertheless, even the so-obtained lower bound for SST material costs is already significantly higher than the LFT counterparts. Therefore, and because of the lower efficiency, a standard TCO consideration will always prefer an LFT due to its lower price and higher efficiency, which translates into lower energy loss costs. Furthermore, the initially mentioned general notion according to which SSTs feature significantly lower weight and volume when compared to LFTs needs to be brought into question again when referring to direct replacements of LFTs by SSTs (cf. Fig. 11(a)).

On the other hand, in grid applications—in contrast to traction—weight and volume usually are not critical constraints. Furthermore, as power electronic system with an inherently high functionality, an AC/AC SST can replace more equipment than only an LFT, e. g., a LFT plus a voltage regulator or a STATCOM device. SSTs can act as power quality providers and even avoid the need of increasing feeder capabilities (which might seem necessary as a result of increasing penetration of photovoltaic infeed on lower voltage levels) due to their ability of controlling the voltage independent of power flow direction. Also, SSTs enable controlling power flows and thus could act as the “energy routers” of a future Smart Grid. Quantifying the economical impact of these additional features is virtually impossible on a generic basis, which is the reason for considering only material costs in this paper, which, however, tries to raise the awareness for seeing SSTs not only as isolated, expensive components but as part of a larger system.

An example for how the specific application scenario can change the outcome of the comparison of SST and LFT solutions can be found in more modern applications such as AC/DC operation, where the SST basically acts as a heavy-duty, medium-voltage power supply. There, the SST solution outperforms the LFT-based solution quite clearly regarding volume, weight and also efficiency, which likely justifies higher purchase prices in the long run alone due to loss energy costs being roughly halved.

V. CONCLUSION

This paper provides a comparison of a 1000 kVA three-phase LFT and an equally rated SST with respect to material costs, weight, volume and losses. As a direct AC/AC replacement for an LFT, the SST solution realizes benefits with respect to volume, but on the other hand is significantly less efficient and has at least five times higher material costs. However, SST-based solutions can clearly outperform conventional transformers plus LV rectifier systems in modern AC/DC applications, achieving about half the losses and one third of the weight and volume, respectively.

All in all, SST technology has significant potential also in grid applications, especially with the Smart Grid being heavily promoted and becoming a reality in the foreseeable future, which increases the requirements in terms of flexibility, intelligence and controllability. However, the usefulness of an SST can only be judged in the context of a given application; there is not a general SST solution that fits every need. Current state-of-the-art LFT technology evolved during more than a hundred years, and represents therefore a truly experienced competitor. Thus SSTs, and explicitly also their relation to various application scenarios, regarding both, technical and economical aspects, should be prominently included in any power electronics or energy research agenda.

REFERENCES

- [1] W. McMurray, "Power converter circuits having a high frequency link," U.S. Patent 3,581,212, 1970.
- [2] S. D. Sudhoff, "Solid state transformer," U.S. Patent 5,943,229, 1999.
- [3] M. Kang, P. Enjeti, and I. Pitel, "Analysis and design of electronic transformers for electric power distribution system," *IEEE Trans. Power Electron.*, vol. 14, no. 6, pp. 1133–1141, 1999.
- [4] M. Manjrekar, R. Kieferndorf, and G. Venkataramanan, "Power electronic transformers for utility applications," in *Conf. Rec. IEEE Industry Applications Conf.*, Rome, Italy, 2000, pp. 2496–2502.
- [5] L. Heinemann and G. Mauthe, "The universal power electronics based distribution transformer, an unified approach," in *Proc. 32nd Annu. IEEE Power Electronics Specialists Conf. (PESC)*, Vancouver, Canada, 2001, pp. 504–509.
- [6] E. Ronan, S. Sudhoff, S. Glover, and D. Galloway, "A power electronic-based distribution transformer," *IEEE Trans. Power Del.*, vol. 17, no. 2, pp. 537–543, Apr. 2002.
- [7] S. Dieckerhoff, S. Bernet, and D. Krug, "Power loss-oriented evaluation of high voltage IGBTs and multilevel converters in transformerless traction applications," *IEEE Trans. Power Electron.*, vol. 20, no. 6, pp. 1328–1336, Nov. 2005.
- [8] M. Steiner and H. Reinold, "Medium frequency topology in railway applications," in *Proc. 12th European Conf. Power Electronics and Applications (EPE)*, Aalborg, Denmark, 2007.
- [9] C. Zhao and S. Lewdeni-Schmid, "Design, implementation and performance of a modular power electronic transformer (PET) for railway application," in *Proc. 14th European Power Electronics and Applications Conf. (EPE)*, Birmingham, UK, Sep. 2011.
- [10] D. Dujic, F. Kieferndorf, F. Canales, and U. Drogenik, "Power electronic traction transformer technology," in *Proc. 7th Int. IEEE Power Electronics and Motion Control Conf. (IPEMC)*, Harbin, China, Jun. 2012, pp. 636–642.
- [11] J. Taufiq, "Power electronics technologies for railway vehicles," in *Proc. Power Conversion Conf. (PCC)*, Nagoya, Japan, Apr. 2007, pp. 1388–1393.
- [12] J. Lai and A. Maitra, "Multilevel intelligent universal transformer for medium voltage applications," in *Proc. Industry Applications Conf.*, Hongkong, China, 2005, pp. 1893–1899.
- [13] U. Drogenik, "A 150kW medium frequency transformer optimized for maximum power density," in *Proc. 7th Int. Integrated Power Electronic Systems Conf. (CIPS)*, Nuremberg, Germany, 2012, pp. 2–7.
- [14] M. R. Islam, Y. Guo, and J. Zhu, "A high-frequency link multilevel cascaded medium-voltage converter for direct grid integration of renewable energy systems," *IEEE Trans. Power Electron.*, vol. 29, no. 8, pp. 4167–4182, 2014.
- [15] W. van der Merwe and T. Mouton, "Solid-state transformer topology selection," in *Int. Industrial Technology Conf. (ICIT)*, Gippsland, VIC, Australia, Feb. 2009, pp. 1–6.
- [16] X. She, A. Q. Huang, F. Wang, and R. Burgos, "Wind energy system with integrated functions of active power transfer, reactive power compensation, and voltage conversion," *IEEE Trans. Ind. Electron.*, vol. 60, no. 10, pp. 4512–4524, 2013.
- [17] D. Grider, H. Ryu, L. Cheng, C. Capell, C. Jonas, A. Burk, and M. O. Loughlin, "Advanced SiC power technology for high megawatt power conditioning," presented at the National Institute of Standards and Technology (NIST) High Megawatt Power Conditioning System Workshop, Gaithersburg, MD, USA, 2012.
- [18] R. Burkart and J. W. Kolar, "Component cost models for multi-objective optimizations of switched-mode power converters," in *Proc. Energy Conversion Congr. and Expo. (ECCE)*, Denver, CO, USA, Sep. 2013, pp. 2139–2146.
- [19] R. Degeneff and R. Barss, "Reducing the effect of sags and momentary interruptions: a total owning cost prospective," in *Proc. 9th Int. Harmonics and Quality of Power Conf.*, Orlando, FL, USA, 2000, pp. 397–403.
- [20] P. Balducci, L. Schienbein, T. Nguyen, D. Brown, and E. Fathelrahman, "An examination of the costs and critical characteristics of electric utility distribution system capacity enhancement projects," in *Proc. IEEE Transmission and Distribution Conf. and Expo.*, Dallas, TX, USA, 2006, pp. 78–86.
- [21] Y. Song and J. Li, "Analysis of the life cycle cost and intelligent investment benefit of smart substation," in *Proc. Innovative Smart Grid Technologies Conf. (ISGT Asia)*, Tinajin, China, 2012, pp. 1–5.
- [22] ABB Ltd., "Liquid filled transformers – IEC standard small and medium, rated power < 2500 kVA, HV ≤ 36 kV," [Online]. Available: <http://goo.gl/qZVfJe>, 2010.
- [23] Siemens AG, "Totally Integrated Power – Applikationshandbuch, Kapitel 5," [Online]. Available: <http://goo.gl/berhdL>, 2005.
- [24] SGB SMIT, "Oil distribution transformers," [Online]. Available: <http://goo.gl/ruKcz5>, 2012.
- [25] J. D. Luze, "Distribution transformer size optimization by forecasting customer electricity load," in *Proc. Rural Electric Power Conference (REPC)*, Fort Collins, CO, USA, Apr. 2009, pp. C2–C2–6.
- [26] R. Targosz, F. Topalis, and W. Irrek, "Selecting energy efficient distribution transformers – a guide for achieving least-cost solutions," Polish Copper Promotion Center and European Copper Institute, Tech. Rep., 2008.
- [27] J. E. Huber and J. W. Kolar, "Optimum number of cascaded cells for high-power medium-voltage multilevel converters," in *Proc. Energy Conversion Congr. and Expo. (ECCE)*, Denver, CO, USA, Sep. 2013, pp. 359–366.
- [28] F. Schwarz, "A method of resonant current pulse modulation for power converters," *IEEE Trans. Ind. Electron. Control Instrum.*, vol. IECI-17, no. 3, pp. 209–221, May 1970.
- [29] A. Esser and H.-C. Skudelny, "A new approach to power supplies for robots," *IEEE Trans. Ind. Appl.*, vol. 27, no. 5, pp. 872–875, 1991.
- [30] J. Huber, G. Ortiz, F. Krismser, N. Widmer, and J. Kolar, " η - ρ Pareto optimization of bidirectional half-cycle discontinuous-conduction-mode series-resonant dc/dc converter with fixed voltage transfer ratio," in *Proc. IEEE Appl. Power Electronics Conf. (APEC)*, Long Beach, CA, USA, Mar. 2013.
- [31] RITTAL GmbH & Co. KG, "Rittal Handbuch 33," [Online]. Available: <http://goo.gl/5TODyb>, 2013.
- [32] J. Kolar, H. Ertl, and F. Zach, "Influence of the modulation method on the conduction and switching losses of a PWM converter system," *IEEE Trans. Ind. Appl.*, vol. 21, no. 6, pp. 1063–1075, 1991.
- [33] U. Drogenik, G. Laimer, and J. Kolar, "Theoretical converter power density limits for forced convection cooling," in *Proc. 26th Int. Power Electronics, Intelligent Motion, Power Quality Conf. (PCIM)*, Nuremberg, Germany, Jun. 2005, pp. 608–619.
- [34] M. Schweizer, "System-oriented efficiency optimization of variable speed drives," PhD Thesis, ETH Zurich, 2012.
- [35] Schneider Electric Power Drives GmbH, Austria, "Datasheets VW3A7257, VW3A7262 and VW3A7267," [Online]. Available: <http://goo.gl/M4QFw8>.
- [36] Schneider Electric Austria Ges.m.b.H., "Schneider Electric Preislisten," [Online]. Available: <http://goo.gl/Bj6IHf>, 2014.